Available online at www.sciencedirect.com

Catalysis Today 98 (2004) 91–98

www.elsevier.com/locate/cattod

Improved hydrogenolysis (C–S, C–M) function with basic supported hydrodesulfurization catalysts

B. Caloch, Mohan S. Rana*, J. Ancheyta

Instituto Mexicano del Petróleo, Hydrotreatment of Maya Crude, Eje Central Lázaro Cárdenas 152, México City 07730, México

Abstract

Hydrotreating (HDT) of model molecules over high specific surface area Co(Ni)Mo/MgO–Al_2O_3 mixed oxide supported catalysts have been investigated for thiophene HDS in a micro-reactor at 400 °C and atmospheric pressure. Thiophene catalytic activity was studied as a function of Mo content (2–16 wt.% Mo), promoter, and support composition [$MgO/(MgO + Al_2O_3)x$ =0.0, 0.01, 0.05, 0.10, 0.50, 1.0]. Supported catalysts were characterized by BET-specific surface area, X-ray power diffraction (XRD), pore volume, and pore size distribution. The promoted molybdenum sulfided catalysts showed a wide range of activity variation with support composition, which establishes that molybdenum sulfided active phases strongly depend on the nature and composition of the support. Maximum activity was observed on sulfided catalysts at $MgO/(MgO + Al_2O_3) = 0.05$. With variation of Mo loading, the activities increase up to 10 wt.% molybdenum loading and after that activity remains constant with further increase in Mo content. The SSA, XRD, and pore volume characterization results are in good agreement with MoO_3 monolayer formation. The incorporation of MgO with γ-Al_2O_3 alters the nature of active phase interaction on the support surface. Therefore, MgO counterpart plays a structural promoting role to the support contribution and its interaction towards the active metal geometry. One lowest composition of MgO (1 wt.% MgO) supported catalyst tested at high pressure with real feed (Maya heavy crude) was compared with a commercial catalyst. The lab prepared catalyst was found to be more stable as well as more active for hydrogenolysis [C–S, C–M (Ni, V)] functions, which were improved by using small amount of MgO with alumina.

Keywords: CoMo; NiMo; HDS; HDM; MgO–Al_2O_3 mixed oxides

1. Introduction

Environmental protection agencies are demanding for improved fuel quality with low sulfur levels. The necessity of lowering the sulfur content, i.e. 50 ppm and below, has led to numerous studies targeted at developing more active catalysts for hydrodesulfurization (HDS) process. In order to deal with these specific targets, a number of studies have been made by changing the support, active phases or incorporation of new promoters in the catalysts [1–6]. The positive role of the support has been discussed in the literature, with interpretations often related to its ability to correctly disperse and provide better morphology to the sulfided phases [7,8]. The use of MgO as a support for hydrotreating (HDT) catalysts has been proposed in literature; however, its commercial application may be limited due to its inherently fragile sensitivity towards water [9–12]. Hydration is one of the serious problems for pure MgO support, since MgO is thermodynamically unstable compared with other HDT supports. MgO reacts very easily with moisture in the air, specially at low coordination sites [13–15], to form $Mg(OH)_2$. Therefore, other supports and binder are needed to incorporate with it and provide a practical support. Alumina is a well-known binder and a support for conventional hydrotreating catalysts. On the other hand, MgO will act as a promoter for support surface properties such as acid-base site generation. Support basicity might be favorable because of increased interaction between support and acidic molybdenum species (MoO_3). Therefore, the use of MgO–Al_2O_3 mixed oxide amorphous and crystalline materials as a basic support can present interesting range of textural properties, which make them potentially attractive as a support for HDT catalysts.

---

* Corresponding author. Tel.: + 52 55 9175 8418; fax: +52 55 9175 8429.
E-mail address: msingh@imp.mx (M.S. Rana).

0920-5861/$ – see front matter © 2004 Elsevier B.V. All rights reserved.
doi:10.1016/j.cattod.2004.07.023

Generally in the literature, MgO-supported sulfide catalysts were reported to be less active for hydrotreating reactions than conventional γ-Al_2O_3 supported catalysts [6,16–18], probably because the high surface area of magnesia is transformed to low surface area magnesium hydroxide during the aqueous impregnation. It is also reported by Klimiova et al. [18] that particularly Ni interacts with the MgO surface and reduces the promotional effect for HDS activity. However, Chary et al. [19] reported that Mo was better dispersed on MgO, when Mo/MgO was prepared by aqueous impregnation, and that sulfided catalysts exhibited a slightly higher activity for thiophene HDS than sulfided Mo/γ-Al_2O_3 catalysts. Several papers published by Zdražil et al. [12,20,21] reported the preparation of pure magnesia supported NiMo(CoMo) catalysts using a non-aqueous impregnation method. They found that the activities of NiMo/MgO catalysts increase several fold compared with a commercial NiMo/γ-Al_2O_3 catalyst at 320 °C.

The aim of this study is to understand the role of MgO–Al_2O_3 mixed oxides support compositions, pore characteristics, and its effect on hydrotreating reactions. The prime objective of the work is to identify a support material, which structurally promotes the catalytic functionalities by modifying the metal support interactions. The results of catalytic properties are evaluated with thiophene hydrodesulfurization as well as with heavy oil (Maya crude) HDS and hydrodemetallization (HDM).

2. Experimental

The MgO–Al_2O_3 supports were prepared according to the homogeneous precipitation method using aqueous aluminum nitrate (2 M), magnesium nitrate (2 M), 10% solution of NH_3 (NH_4OH) as a precipitating agent and controlling the precipitation at pH $\approx$ 10 in presence of stirring. The stirring was continuous for 4 h to allow the complete mixing of precipitation of two dissimilar oxides. The precipitation was digested overnight ($\sim$15 h) and filtered with the required amount of distilled water to wash the nitrate ions. The vacuum dried cake was used to prepare wet extrudates. The extrudates were then dried at room temperature, 120 °C, and finally calcined at 550 °C for 4 h. The samples with varying MgO–Al_2O_3 ratios were prepared by adjusting the amounts of the aluminum nitrate and magnesium nitrate concentrations. These samples are labeled as AM-0.01 (1 wt.% MgO-99 wt.% Al_2O_3), AM-0.05 (5 wt.% MgO-95 wt.% Al_2O_3), AM-0.10 (10 wt.% MgO-90 wt.% Al_2O_3), and AM-0.50 (50 wt.% MgO-50 wt.% Al_2O_3). Pure MgO and γ-Al_2O_3 were also prepared according to a similar procedure.

The molybdenum-supported catalysts were prepared by the incipient wetness impregnation method. An appropriate amount of ammonium heptamolybdate (AHM) (Fluka AR grade) was dissolved in NH_4OH solution for impregnation. The Co- and Ni-promoted catalysts were prepared by sequential impregnation procedure on Mo-supported catalysts (dried 120 °C and calcined at 400 °C). The cobalt and nickel nitrate salts were impregnated in aqueous medium. The final catalysts were dried in air at 120 °C overnight, and calcined at 450 °C for 4 h.

The BET SSA, pore volume, and PSD were carried out in a Quantochrome Nova 2000 equipment. Nitrogen gas was employed for SSA measurements at liquid nitrogen temperature (−196 °C). Prior to the adsorption, the samples were out-gassed 3 h at 300 °C. X-ray power diffraction (XRD) patterns were collected on a Siemens D500 diffractometer in a 2θ range 5–70° at 2.5° min^{-1} scan rate using the Cu Kα radiation.

The catalytic activity of supported and promoted catalysts was evaluated for the hydrodesulfurization of thiophene at 400 °C. In a typical experiment, about 200 mg ($\pm$10 mg) of catalyst sample (0.2–0.5 mm grain size) was secured between two plugs of quartz wool inside the reactor (Pyrex glass tube, 0.8 cm i.d.). Prior to the activity test, the catalyst was sulfided at 400 °C for 2 h in a flow rate of 50 ml/min, of a CS_2/H_2 mixture (10 % CS_2 and 90 % H_2) in a fixed bed reactor operating at atmospheric pressure. After sulfidation, thiophene HDS experiments were conducted at 400 °C with $\sim$100 ml/min flow (keeping W/F constant) of hydrogen through a thiophene saturator at 20 °C. The products were analyzed online using a FID gas chromatography. The conversions of thiophene were kept below 12% to operate in differential regime. Thiophene conversion data were collected at 30-min intervals over 4 h. Catalyst activities reported here are the value of steady state after 4 h time on-stream. Reaction rates were calculated according to the equation $r = x\,(F/W)$, where r is the reaction rate of thiophene in mol/h/g, x is the conversion, W is the weight of the catalyst in grams, and F is the initial flow rate of the reactant in mol/h. First order rate of reaction was considered for thiophene conversion.

To evaluate the catalytic behavior with real feed one catalyst (CoMo/AM-0.01) was tested on high pressure micro reactor described elsewhere [22]. The feed for this experiment was prepared synthetically with hydrodemetallized (HDM) Maya crude and diesel (50/50, w/w). Diesel was used as solvent to avoid precipitation as well as gum formation during the feed processing. The properties of the feed are presented in Table 1. Metals (Ni, V) in the feed and products were analyzed using flame atomic adsorption spectrometry (D 5863-00a ASTM standard). The sulfure content was analyzed by ultra-violate fluorescence (D 5453-00 ASTM standard), while nitrogen was measured by oxidative combustion and chemiluminescence (D 4629-02 ASTM standard) at high temperature combustion in an oxygen-rich atmosphere. Asphaltene is defined as the insoluble fraction in *n*-pentane.

The catalyst pretreatment and the hydrotreating reactions were carried out in the high-pressure fixed bed flow reactor. The catalyst was sulfided in situ with a mixture of dimethyldisulfide (DMDS), straight run gas oil (SRGO), and H_2

Table 1
Characterization of feed for high-pressure experiments

Properties	HDS feed
Density (20/4 °C)	0.8505
Asphaltene (nC_5 insol.) (wt.%)	6.36
Elemental analysis (wt.%)	
C	83.2
H	9.5
N	0.1325
S	2.16
Metal (wppm)	
Ni	25.04
V	86.84
Ni + V	111.88

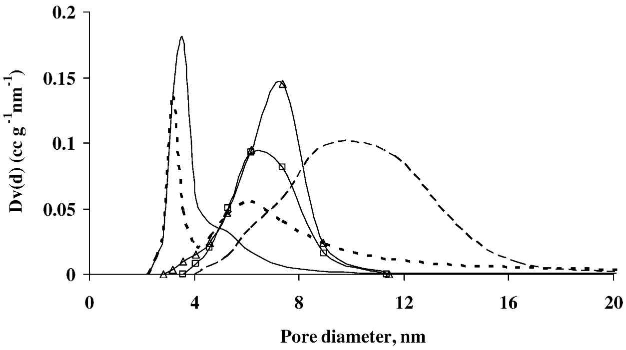

Fig. 1. Pore size distribution of Al_2O_3, MgO, and $MgO–Al_2O_3$ supports: (——) γ-Al_2O_3; (- - -) AM-0.01; (– – –) AM-0.05; (Δ) AM-0.10; (□) AM-0.50.

(1 wt.% DMDS + SRGO). The H_2S is produced by decomposition of DMDS in situ. The reactor was loaded with around 10 ml volume of oxided catalyst with 3–5 mm extrudates size diluted with equal volume of SiC. After depressurizing the reactor to atmospheric pressure, the sulfiding stream containing ≈2.0 wt.% "S" was fed to wet the catalyst bed at room temperature. The reactor liquid was drained after 4 h and then temperature linearly rose from 30 to 120 °C (30 °C/h) and kept at this temperature for 2 h. The temperature was then increased until 150 °C at the rate of 30 °C/h, at pressure of 2.8 MPa, and stayed 2 h, further increase in temperature at 260 °C and hold for 3 h. The final temperature of sulfidation was 320 °C, and stabilizes for 5 h at 2.8 MPa. After sulfidation, the flow was switched to HDS feed (Table 1) and the following operating conditions were adjusted: temperature of 380 °C, LHSV of 1 h^{-1}, H_2/HC 356 m^3/m^3, and pressure of 5.4 MPa [23].

3. Results and discussion

2.1. Support properties

$MgO–Al_2O_3$ mixed oxides prepared with co-precipitation method provide good textural properties of support. The calcined solids were produced with high SSA and mesoporous in nature as can be seen in Table 2 and Fig. 1, respectively. Pure MgO displayed a very low specific area (50 m^2/g) in comparison with $MgO–Al_2O_3$ mixed oxides, which fall in the range of 120–220 m^2/g. The mixed oxide SSA increases up to 1 wt.% MgO after that SSA decreases with further increasing of MgO content due to the contribution of MgO, which itself has low SSA. The N_2 adsorption–desorption curves correspond to the Type IV isotherm, characteristic of mesoporous materials. However, pure alumina presents a relatively narrow pore size distribution (PSD) centered at 4–6 nm, whereas the mixed oxides PSD are slightly broader and centered between 5–15 nm depending on the MgO contribution. The variation in pore size distribution with the effect of support composition may depend on the alumina and MgO interaction (Mg–Al–O) and the growth of crystal formation during the preparation, which establishes the relationship with pores size distribution, SSA and total pore volume. The minimum pore broadening obtained in the case of AM-0.50 may be due to the MgO–MgO interaction increase and bigger crystal formation, which decrease the SSA as well as pore volume [24]. On the other hand, the PSD in AM-0.01 is very similar to pure alumina.

The XRD patterns for pure γ-Al_2O_3, MgO, and mixed oxide ($MgO–Al_2O_3$) supports were recorded between 5 and 70° 2θ values of Joint Committee on Powder Diffraction Standards (JCPDS) [25] for γ-Al_2O_3, and MgO solids are compared with the mixed oxides crystalline phases in Fig. 2.

Table 2
Characterization and composition of support and supported catalysts

	MgO/(MgO + Al_2O_3)	Support		Catalysts			
		SSA (m^2/g)	PV (ml/g)	Mo (%)	Co (Ni) (%)	SSA (m^2/g)	PV (ml/g)
γ-Al_2O_3	0.0	209	0.27	7.9	2.4	170	0.18
AM-0.01	0.01	212	0.40	7.9	2.3	182	0.31
AM-0.05	0.05	185	0.52	7.8	2.3	161	0.41
AM-0.10	0.10	179	0.41	8.0	2.4	153	0.30
AM-0.50	0.50	116	0.28	7.7	2.3	75	0.13
MgO	1.00	50	0.13	7.8	2.2	13	0.52
CC-1		–	–	12.3	2.7 (0.7)	266	0.48
CC-2		(γ-Al_2O_3 + 5.6% Ti)		11.5	2.9	152	0.37

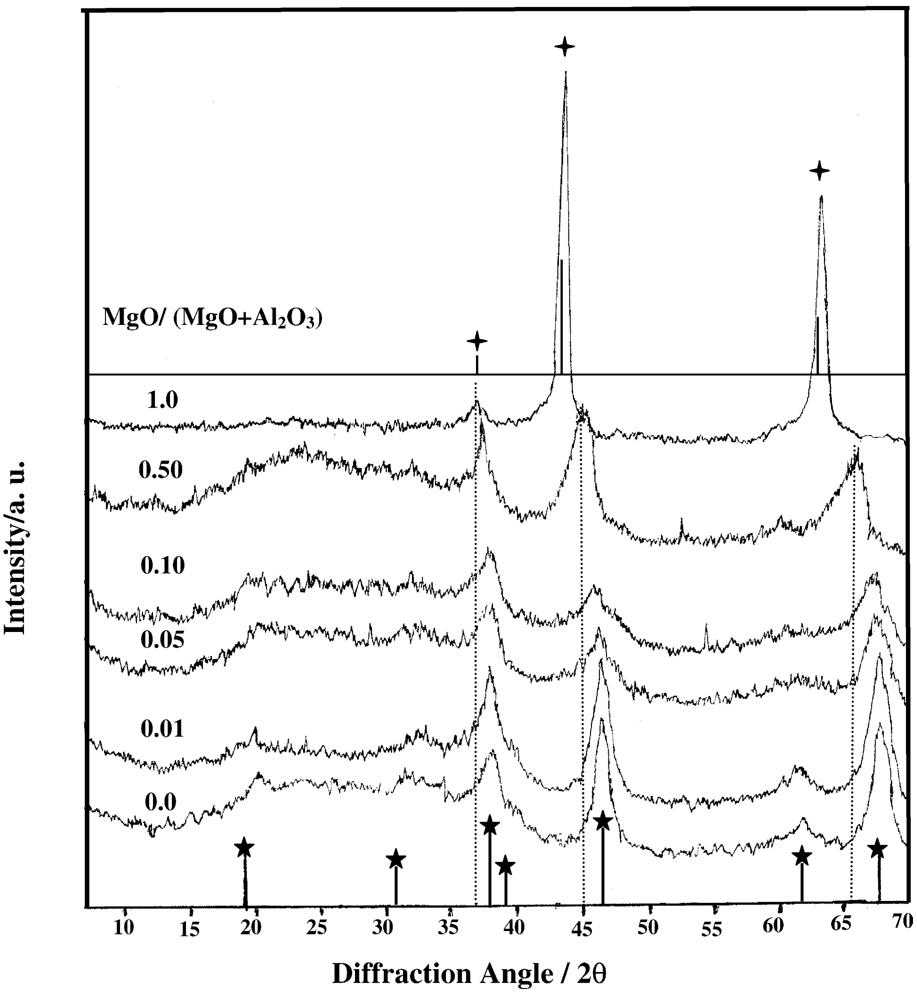

Fig. 2. X-ray diffractograms of MgO–Al_2O_3 mixed oxides and comparison with ASTM data: (★) γ-Al_2O_3-JCPD file number 10–425; (✦) MgO-JCPD file number 064930.

The XRD results represent the variation of support composition, the intensity of MgO phase increases with MgO content particularly in the case of x = 0.50 mixed oxide. The lowest MgO containing sample (x = 0.01) exactly looks like pure γ-Al_2O_3, but when the MgO content increases the 2θ value is shifting toward the MgO and the intensity [2θ = 33, 45, and 66] becomes more prominent.

2.2. Catalysts characterization

The Mo-supported catalysts and their Co-promoted analogues were characterized in the oxide state by BET SSA, pore volume, PSD, and XRD measurements. It can be seen from Table 2 that specific area decreases by impregnation of cobalt and molybdenum. However, MgO ($x > 0.10$) is more sensitive to the ambient conditions. Therefore, the decrease in SSA is more apparent in the case of higher MgO containing supports. Hence, aqueous impregnation of low MgO containing support ($x \leq 0.10$) does not affect the textural properties of support. The SSA measured as a function of Mo loading viz. surface area per gram of support and catalysts are shown in Fig. 3 for Mo/AM-0.05. The surface area per gram of catalyst decreases with increasing Mo loading, while the surface area per gram of support remains constant up to 10 wt.% Mo loading and then decreases with further increasing of Mo content. Similar results were

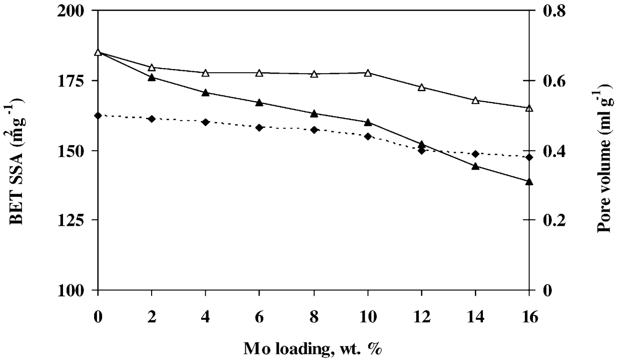

Fig. 3. Variation in specific surface area and total pore volume as a function of Mo loading on AM-0.05: (Δ) surface area per gram of support; (▲) surface area per gram of catalyst; (◆) pore volume.

obtained by Massoth [26]. This information could reflect about the MoO_3 dispersion or its monolayer formation. In the case of monolayer formation of an oxide on the surface of support, the area should remain constant. The results show that MoO_3 is in dispersed state up to 10 wt.% Mo. The decrease in SSA after 10 wt.% Mo loading may indicate pore blockage due to the bigger crystal formation of MoO_3. The decrease in pore volume also represents similar kind of results. The XRD results also agreed with this conclusion that Mo is well dispersed on the high surface area supports up to 10 wt.%. The XRD results are presented for Mo/AM-0.05 as a function of Mo loading in Fig. 4, there are some (d = 7.014, 3.83, and 3.28) indications for crystalline phases due to the presence of MoO_3, which further revealed that Mo is well dispersed up to 10 wt.% or the crystal size of Mo is less than 4 nm.

2.3. *Catalytic activity for thiophene HDS*

2.3.1. *Effect of Mo content*

The activity of sulfided catalysts was evaluated in thiophene hydrodesulphurization. The rates of thiophene disappearance plotted as a function of Mo loading are presented in Fig. 5. The Mo supported catalysts activity increases more or less linearly with increasing Mo loading up to 10 wt.%, and then remains constant with further increase in Mo loading. In general, this variation of thiophene HDS with the Mo content is closely related to the variation with Mo dispersion on the support surface. The initial linear increase of HDS activity reflects the amount of sulfur vacancies (anion vacancies or coordinative unsaturated sites) created on the sulfided catalysts, in which HDS reaction takes place. The HDS rate stands constant after 10 wt.% Mo loading, which represents that above this loading, the formation of Mo multilayer occurred leading to a decrease in HDS activity. These activity results are in good agreement with the surface area and pore volume decrease.

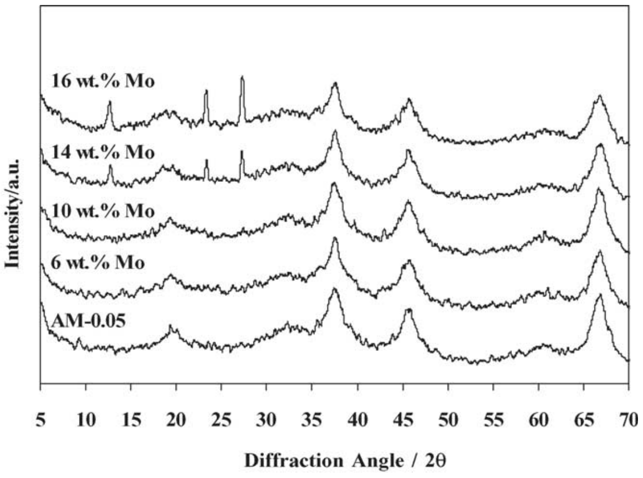

Fig. 4. X-ray diffractogram of Mo supported (AM-0.05) catalysts.

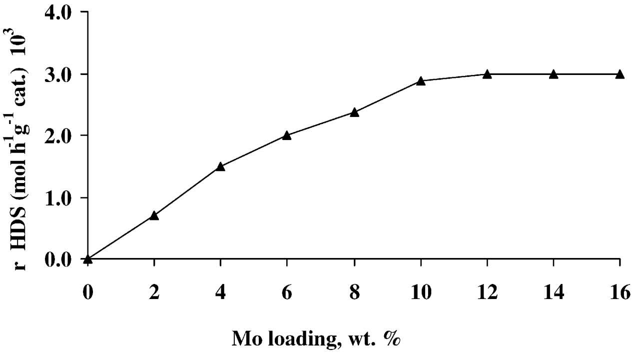

Fig. 5. Variation of thiophene rate as a function of Mo loading.

2.3.2. *Effect of support composition*

In order to assess the support effect on hydrotreating catalyst, thiophene HDS activity was carried out as a function of MgO content. A comparison of γ-Al_2O_3 and MgO supported catalysts is also shown in Fig. 6. These catalysts contain 8 wt.% Mo and 2.4 wt.% Co, having Co/(Co + Mo) molar ratio of 0.32. Pore size distribution of mixed oxides, specially in the case of x = 0.0,0.01, 0.05, and 0.10 after Co–Mo loading (Fig. 7), showed similar type of profile and only the pore volume decreased slightly due to the deposition of active metals (Table 2). Therefore, there are not many changes occurred in textural properties due to the aqueous impregnation with low concentration of MgO ($x \leq 0.1$) in the support, while for pure MgO (x = 1.0) the PSD profile changes completely as can be seen in Fig. 7 inset. The changes in the case of pure MgO texture are due to the dissolution of MgO during the aqueous impregnation, which results in the removal of thin wall between the meso-porous of MgO, a reaction that leads to the formation of large (macro) pores. These results vary with already reported results [10,18] about the dissolution of the MgO during the aqueous impregnation, particularly when low MgO content was mixed with alumina. Hence, the MgO–Al_2O_3 ($x \leq 0.10$) is chemically and texturally stable in aqueous impregnation of Co and Mo salts. However, the interactions of Ni (Co) to the MgO support remain unexplained from these results. To appreciate the role of support composition, thiophene activity on different supported catalysts will reveal the

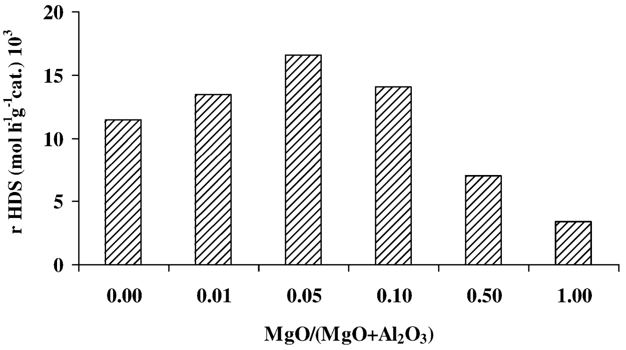

Fig. 6. Comparison of HDS rate as a function of support composition.

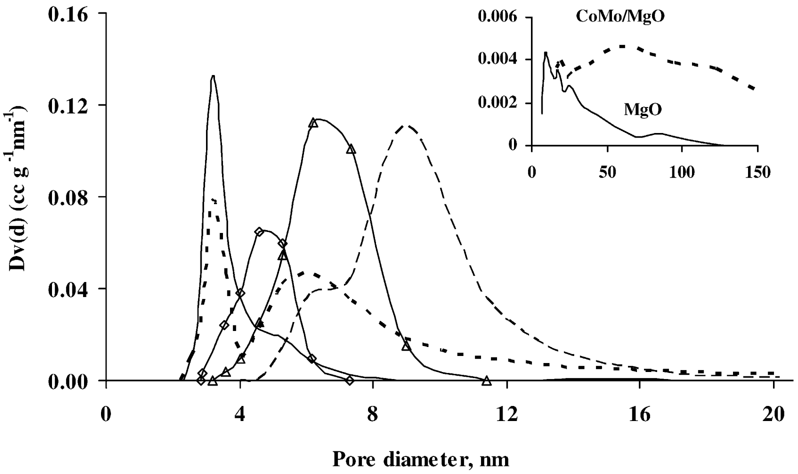

Fig. 7. Pore size distribution of CoMo supported catalysts: (——) CoMo/γ-Al_2O_3; (- - -) CoMo/AM-0.01; (– – –) CoMo/AM-0.05; (Δ) CoMo/AM-0.10; (◇) CoMo/AM-0.50.

possible role of support modifications towards active phase interactions in sulfided catalysts. These results indicate that the maximum HDS activity is obtained at CoMo/AM-0.05 and with further increase of MgO content the activity decreases rapidly as shown in Fig. 6. According to our results we conclude that this is the maximum amount of MgO, which is dispersed in alumina and does not lead to any disadvantage during the aqueous impregnation or catalyst preparation. Moreover, an increase of MgO content may precipitate as MgO bigger particle, which decrease the surface area as well as dispersion of active metals [27].

2.3.3. *Effect of CoMo and NiMo supported catalyst*

To understand the effect of the Co and Ni promoters on thiophene HDS in the Mo/MgO–Al_2O_3 (AM-0.05) system, the concentration of the promoters were kept constant for Ni and Co, i.e. Co(Ni)/[Co(Ni) + Mo] = 0.37. The activity data were compared for Mo, CoMo, NiMo, and a commercial catalyst (CC-1), as shown in Fig. 8. It can be seen from the figure that there is a significant effect on MgO containing support (AM-0.05). To compare the effect of Co/(Co + Mo) molar ratio, we varied it at 0.32 and 0.37, and we observed that 0.32 showed better HDS rate than 0.37 (16.6 versus 13.8 mol/h/g cat.). The promoted catalysts showed four to six times higher activity than Mo supported catalysts; this large promotional effect contradicts the previous results presented by Klimiova et al. [18] since they found moderate promotional effect for Ni at Ni/(Ni + Mo) atomic ratio of 0.30, while with increasing the ratio up to 0.6, they observed higher promotional effect which may be due to the higher calcination temperature at 500 °C that might increase the possibility of interaction between NiO and MgO support. In our study, the final catalysts were calcined at 450 °C for 4 h. However, our CoMo and NiMo promoted catalysts results are in good agreement with Zdražil and co-workers [10–12]. The promoted catalysts were compared with a commercial catalyst and we found that CoMo/MgO–Al_2O_3 promoted catalysts are comparable or slightly better at our reaction conditions, while NiMo are slightly inferior to the commercial catalyst. The effect of Ni or Co on MgO containing support shows that CoMo is better catalyst than NiMo, which is more similar to the conventional alumina supported catalyst.

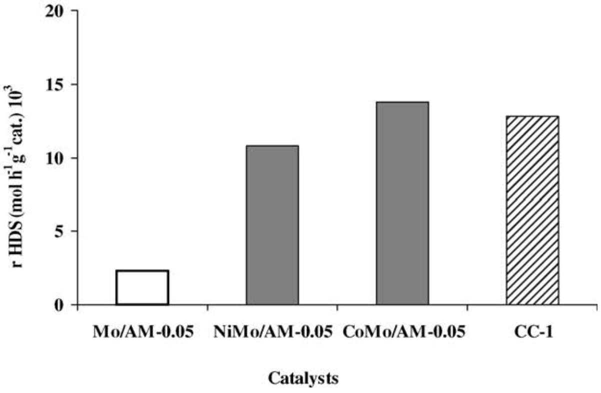

Fig. 8. Effect of promoters (Co or Ni) on HDS activity of thiophene.

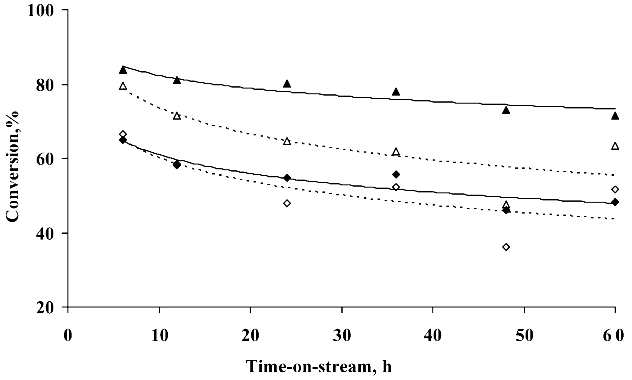

Fig. 9. HDS and HDM conversions with time on-stream: (▲) CoMo/AM-0.01 HDS; (△) CC-2 HDS; (◆) CoMo/AM-0.01 HDM; (◇) CC-2 HDM.

2.3.4. Catalytic activity for Maya crude

In order to consider the catalytic behavior of MgO added catalyst (CoMo/AM-0.01) in heavy oil hydrotreating under H_2 pressure (5.4 MPa), the relative reaction conversion for HDS and HDM are shown in Fig. 9, and the results are compared with a commercial catalyst (CC-2) in same the figure. The compositions of these catalysts are reported in Table 2. The selection of the lowest MgO containing support for this study was to prepare more stable support where MgO plays a role of neutralizer to acid site keeping other silent features from alumina support. Recently, Aberuagba et al. [24] presented the acidity and cumene cracking activity on $MgO–Al_2O_3$; they studied the MgO content of 25, 50, and 75 wt.% with alumina and reported a decrease in acidity with MgO increase.

The $MgO–Al_2O_3$ supported catalyst presented clearly better activity for HDS of Maya crude as well as more stable activity with time on-stream. However, in the case of parallel HDM, reaction activity and stability were slightly better or equal than those found with the commercial catalyst. It seems that larger pores in commercial catalyst (Fig. 10) play an important role to make this difference in HDS and HDM activities. The better HDS and HDM activities for CoMo/AM-0.01 catalyst may be due to the effect of MgO in the support in agreement with the basic supported catalysts, which are more active to the hydrogenolysis [C–S or C–M (Ni, V)] and less hydrogenative in nature [1]. Therefore, the small amounts of MgO may encrust on the alumina surface and indeed promote the support nature towards the better geometry of active phases. Shimada et al. [6] reported a significant support effect on the hydrogenolysis functionalities, which strongly depends on the two-dimensional polymolybdate structure of active phases. For HDS, the active sites are considered more important than the textural properties of support, while for HDM, the textural properties as well as active sites seem to be important due to the diffusion of organo-metallic complex molecule into the pores. With respect to the effect of time on-stream, MgO containing supported catalyst is more stable than the commercial one. Eijsbout et al. [28] suggested that HDS deactivation is due to the loss of the active phase during the hydrotreating reaction. The catalytic performance and the service life of the catalyst are directly related to the dispersion of the active phases. On the other hand, Gosselink [29] reported that during heavy oil hydro-conversion the metal sulfide deposition is taking place on the pore mouth; therefore an increase in the pore diameter increases the metal tolerance, but decreases the surface area and thus the activity. Hence, with regard to the heavy oil processing the balance between the two independent parameters (dispersion and textural properties) of the MgO supported catalysts is an invitation for further detail investigation on the characterization as well as activity tests.

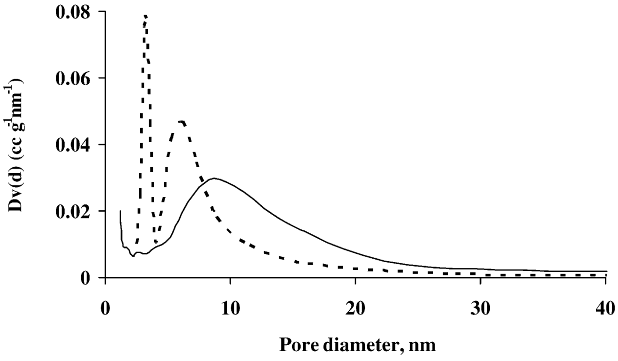

Fig. 10. Pore size distribution of CoMo/AM-0.01 and commercial catalyst: (——) CC-2; (- - -) CoMo/AM-0.01.

3. Conclusions

High specific surface area $MgO–Al_2O_3$ support can be prepared using coprecipitation method. The loss of specific surface area using aqueous impregnation on $MgO–Al_2O_3$ with high alumina containing support was limited, and the hydration resistance was much superior to pure MgO support. The comparison with alumina supported catalysts revealed that MgO containing ($x = 0.05$) supported catalysts are more active for thiophene HDS. Lower amount of MgO in alumina ($x \leq 0.10$) support showed stable behavior in aqueous solution of Co and Mo salts. In the variation of promoters (Co/Ni) on $MgO–Al_2O_3$ (AM-0.05) supported catalysts, CoMo represents better activity than NiMo for thiophene HDS. The high-pressure HDT results on supported catalysts indicated that the introduction of MgO in the Al_2O_3 provides higher hydrogenolysis function (HDS and HDM) and more stable behavior with time on-stream due to the basic nature of support. In other words mixing of MgO with Al_2O_3 modifies the interaction behavior of support towards the active phases and consequently increases the activity.

Acknowledgements

B. Caloch thank for financial support for a graduate thesis grant, and M.S. Rana thank for the Instituto Mexicano del Petroleo (Mexico) for providing PDF. We also express our appreciation to Mr. Jose G. Espinosa and Mrs. Bertha Nuñez for helping in the construction of micro-plant and adsorption–desorption experiments.

References

[1] H. Topsøe, B.S. Clausen, F.E. Massoth, in: J.R. Anderson, M. Boudart (Eds.), Hydrotreating Catalysis – Science and Technology, 11, Springer-Verlag, New York, 1996.
[2] M. Breysse, J.L. Portefaix, M. Vrinat, Catal. Today 10 (1991) 489.
[3] T.A. Pecoraro, R.R. Chianelli, J. Catal. 67 (1981) 430.
[4] G. Murali Dhar, M.S. Rana, S.K. Maity, B.N. Srinivas, T.S.R. Prasada Rao, Chemistry of Diesel Fuels, 2000 Chapter 8.

[5] U.T. Turaga, C. Song, ACS Div. Petroleum Chem. Prep. 47 (2002) 97.
[6] H. Shimada, T. Sato, Y. Yoshimura, J. Hiraishi, A. Nishijima, J. Catal. 110 (1988) 275.
[7] M.A.M. Bouwens, J.P.R. Vissers, V.H.J. de Beer, R. Prins, J. Catal. 112 (1988) 401.
[8] M.S. Rana, S.K. Maity, J. Ancheyta, G. Murali Dhar, T.S.R. Prasada Rao, Appl. Catal. A 253 (2003) 165.
[9] E. Holt, A.D. Logan, S. Chakraborti, A.K. Datye, Appl. Catal. A Gen. 34 (1987) 199.
[10] T. Klicpera, M. Zdražil, J. Catal. 206 (2002) 314.
[11] T. Klicpera, M. Zdražil, Catal. Lett. 58 (1999) 47.
[12] T. Klicpera, M. Zdražil, Catal Appl. A 216 (2001) 41.
[13] M.O. Aboelfotos, K.C. Park, W.A. Pliskin, J. Appl. Phys. 48 (1977) 2910.
[14] Y. Kuroda, E. Yasugi, H. Aoi, K. Miura, T. Morimoto, J. Chem. Soc. Faraday Trans. 1 (84) (1988) 2421.
[15] C.A. Scamehorn, N.M. Harrison, M.I. McCarthy, J. Chem. Phys. 102 (2) (1994) 1547.
[16] R.J. Bertolacini, A.-Quan-Sue, A. Trevelyan, U.S. Patent 4,140, 626.
[17] H. Hattori, K. Yamashita, K. Kobayashi, T. Tanabe, K. Tanabe, in: J.A. Mouljin, K.N. Nater, H.A.G. Chermin (Eds.), in: Proceedings of the 1987 International Conference on Coal Science, Elsevier, Amsterdam, 1987, p. 285.
[18] T. Klimiova, D.S. Casados, J. Ramirez, Catal. Today 43 (1998) 135.
[19] K.V.R. Chary, H. Ramakrishna, K.S. Rama Rao, G. Murali Dhar, P. Kanta Rao, Catal. Lett. 10 (1991) 27.
[20] E. Hillerova, Z. Vit, M. Zdražil, Catal Appl. A 118 (1994) 111.
[21] J. Cinibulk, P.J. Kooyman, Z. Vit, M. Zdražil, Catal. Lett. 89 (2003) 147.
[22] L.C. Castañeda, F. Alonso, J. Ancheyta, Stud. Surf. Sci. Catal. 133 (2001) 477.
[23] S.K. Maity, J. Ancheyta, L. Soberanis, F. Alonso, M.E. Llanos, Catal Appl. A 244 (2003) 141.
[24] F. Aberuagba, M. Kumar, J.K. Gupta, G. Murali Dhar, L.D. Sharma, React. Kinet. Catal. Lett. 75 (2002) 245.
[25] Powder Diffraction Files, JCPDS, International Central for Diffraction Data, 1969.
[26] F.E. Massoth, J. Catal. 36 (1975) 166.
[27] J.F. Le Page, et al., in: Applied Heterogeneous Catalysis, Design, Manufacture, Use of Solid Catalysts, Technip, Paris, 1987, p. 203.
[28] S. Eijsbout, J.J.L. Heinerman, H.J.W. Elzerman, Appl. Catal. A 105 (1993) 69.
[29] J.W. Gosselink, CatTech 2 (1998) 127.